Kobe University Repository : Kernel

PDF issue: 2025-12-04

Charge-carrier dynamics in benzoporphyrin films investigated by time-resolved terahertz spectroscopy

Ohta, Kaoru
Hiraoka, Sho
Tamura, Yuto
Yamada, Hiroko
Tominaga, Keisuke

(Citation)
Applied Physics Letters,107(18):183302-183302

(Issue Date)
2015-11-02

(Resource Type)
journal article

(Version)
Version of Record

(Rights)
©2015 American Institute of Physics. This article may be downloaded for personal use only. Any other use requires prior permission of the author and the American Institute of Physics. The following article appeared in Applied Physics Letters 107(18), 188302 and may be found at http://dx.doi.org/10.1063/1.4934690

(URL)
https://hdl.handle.net/20.500.14094/90003258

AIP Applied Physics Letters

Charge-carrier dynamics in benzoporphyrin films investigated by time-resolved terahertz spectroscopy

Kaoru Ohta, Sho Hiraoka, Yuto Tamura, Hiroko Yamada, and Keisuke Tominaga

Citation: Applied Physics Letters **107**, 183302 (2015); doi: 10.1063/1.4934690
View online: http://dx.doi.org/10.1063/1.4934690
View Table of Contents: http://scitation.aip.org/content/aip/journal/apl/107/18?ver=pdfcov
Published by the AIP Publishing

Articles you may be interested in

Employing time-resolved terahertz spectroscopy to analyze carrier dynamics in thin-film Cu2ZnSn(S,Se)4 absorber layers
Appl. Phys. Lett. **104**, 253901 (2014); 10.1063/1.4884817

Charge carrier dynamics in organic semiconductors and their donor-acceptor composites: Numerical modeling of time-resolved photocurrent
J. Appl. Phys. **114**, 094508 (2013); 10.1063/1.4820259

Size and surface effects on transient photoconductivity in CdS nanobelts probed by time-resolved terahertz spectroscopy
Appl. Phys. Lett. **101**, 091104 (2012); 10.1063/1.4748300

Carrier dynamics and conductivity of SnO2 nanowires investigated by time-resolved terahertz spectroscopy
Appl. Phys. Lett. **100**, 133101 (2012); 10.1063/1.3698097

Morphology effects on charge generation and recombination dynamics at ZnPc:C60 bulk hetero-junctions using time-resolved terahertz spectroscopy
Appl. Phys. Lett. **99**, 143304 (2011); 10.1063/1.3644129

Reuse of AIP Publishing content is subject to the terms at: https://publishing.aip.org/authors/rights-and-permissions. IP: 133.30.52.203 On: Mon, 22 Feb 2016 02:05:38

Charge-carrier dynamics in benzoporphyrin films investigated by time-resolved terahertz spectroscopy

Kaoru Ohta,[1] Sho Hiraoka,[2] Yuto Tamura,[3] Hiroko Yamada,[3,4] and Keisuke Tominaga[1,2]
[1]*Molecular Photoscience Research Center, Kobe University, 1-1 Rokkodai-cho, Nada, Kobe 657-8501, Japan*
[2]*Graduate School of Science, Kobe University, 1-1 Rokkodai-cho, Nada, Kobe 657-8501, Japan*
[3]*Graduate School of Materials Science, Nara Institute of Science and Technology, 8916-5 Takayama-cho, Ikoma, Nara 630-0192, Japan*
[4]*CREST, Japan Science and Technology (JST), 4-1-8 Honcho, Kawaguchi, Saitama 332-0012, Japan*

(Received 12 July 2015; accepted 11 October 2015; published online 2 November 2015)

We investigated charge-carrier dynamics in benzoporphyrin (BP) and BP-based bulk heterojunction (BHJ) films with optical pump-broadband terahertz (THz) probe spectroscopy. In both samples, we observed instantaneous appearance of transient THz signals, which are attributed to mobile charge carriers that are much lower in transition energy than excitons. These carriers recombine and/or trap at defect sites within a few ps. In the BP-based BHJ films, the decay dynamics of transient THz signals was faster relative to that in the BP films. In contrast to the BP films, approximately 10% of the transient signal does not decay within 35 ps, indicating survival of free charge carriers. © *2015 AIP Publishing LLC*. [http://dx.doi.org/10.1063/1.4934690]

Conjugated organic semiconductors have been extensively studied because of promising applications in field-effect transistors and solar cells.[1–3] One of the reasons for widespread interest is that solution processing can be used for fabrication of photovoltaic devices. Conjugated polymers such as poly(3-hexylthiophene) (P3HT) and related compounds are the most commonly used organic semiconductors. Bulk heterojunction (BHJ) structures, where polymers are blended with acceptor molecules, improve charge separation and transport processes for increased power conversion efficiency.[1,2] Another important class of compounds includes phthalocyanines and porphyrins, which also have excellent optical and electronic properties.[3–5] In contrast to polymers, they have the flexibility of varying functional groups and structures and can form thin films with a high degree of crystallinity and structural order.[6,7]

To optimize power conversion efficiency, it is important to understand the detailed mechanisms of charge generation, recombination, and charge–carrier mobilities.[8] Ultrafast time-resolved spectroscopic methods probe charge-carrier dynamics in real time. In particular, transient absorption (TA) measurements have been used to examine fundamental processes in organic photovoltaics. Even though TA monitors charge-carrier dynamics with high sensitivity and high time resolution, the spectral assignments are sometimes not straightforward because the electronic transitions are not directly related to the motion of the charge carriers.[9,10]

Recently, time-resolved terahertz (THz) spectroscopy was used to quantify the complex-valued conductivity of charge carriers.[11,12] This is a non-invasive and contact-free method that avoids electrodes and high electric fields for long distance carrier transport. The THz region typically corresponds to scattering rates in semiconductors, which provide detailed information on both carrier density and mobility.[11,12] Most time-resolved THz spectroscopic studies on organic photovoltaic devices have been focused on charge-carrier dynamics in polymer-based systems and dye-sensitized solar cells.[13–21] There have been few studies on small-molecule semiconducting systems, except for polyacenes such as pentacene and rubrene.[22–25]

Heilweil *et al.* have studied photoexcitation dynamics in multi-layer films of zinc phthalocyanine and C_{60}, and found that decay of transient signal in the first 20 ps reflects recombination dynamics.[26,27] However, excitation of neat zinc phthalocyanine films does not yield a signal, indicating that charge transfer from zinc phthalocyanine to C_{60} is required to observe carrier dynamics. Furthermore, short-lived THz photoconductivity is the signature of hot charge carriers, and its magnitude is sensitive to the interfacial volume between donors and acceptors.[28] Charge-carrier dynamics of porphyrin-based organic semiconductors has not been examined with time-resolved THz spectroscopy. Furthermore, in most of previous time-resolved THz studies observed bandwidths are limited to less than 100 cm^{-1}. This is because the generation and detection of the THz pulses are based on the optical rectification and/or electro-optical sampling of ZnTe or GaP crystals, allowing only measurements of the tails of broad featureless spectra to resolve the carrier dynamics.[12–25] Here, we performed optical pump-broadband THz probe measurements to investigate charge carrier dynamics in benzoporphyrin (BP) films and in corresponding BHJ films blended with [6,6]-Phenyl C_{61} butyric acid methyl ester (PCBM).

The time-resolved THz spectrometer was based on a femtosecond laser-induced plasma and air-biased coherent detection.[29–31] Details are presented in the supplementary material.[32] Time dependence of transient conductivity was determined by the change in peak amplitude of the THz waveform as a function of the optical pump-THz probe delay. Transient complex conductivity spectra were acquired by scanning time delays between the optical pump and the THz detection pulses synchronously at a fixed THz probe delay. As shown previously, the time resolution of this scan mode does not depend on the duration of the THz probe

 © 2015 AIP Publishing LLC

Reuse of AIP Publishing content is subject to the terms at: https://publishing.aip.org/authors/rights-and-permissions. IP: 133.30.52.203 On: Mon, 22 Feb 2016 02:05:38

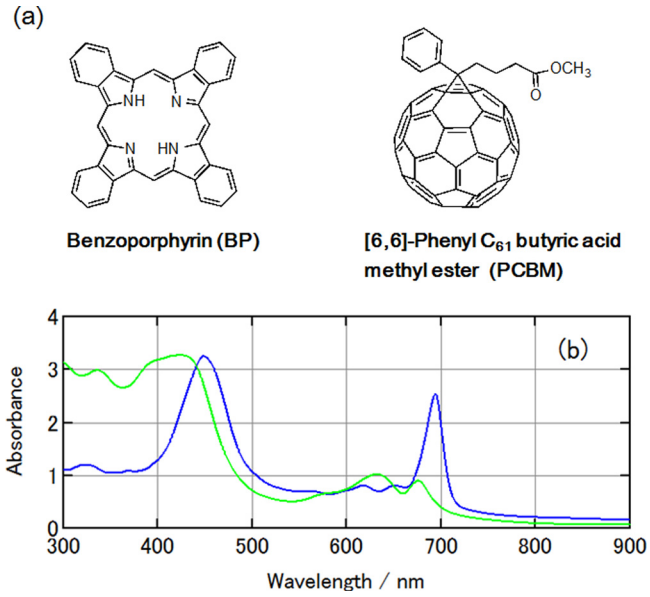

FIG. 1. (a) Molecular structures of benzoporphyrin (BP) and [6,6]-Phenyl C_{61} butyric acid methyl ester (PCBM). (b) Absorption spectra of BP film (blue) and BP:PCBM (1:1) bulk heterojunction (BHJ) film (green).

pulse but on the duration of the optical pump pulse and dispersion in both the generation and detection media.[33] The BP and BP:PCBM (1:1) BHJ films were fabricated on 0.3 mm thick fused silica substrates, as described.[7]

Figure 1 plots the UV-visible absorption spectra of BP and BP:PCBM BHJ films along with their molecular structures. In the BP film, Soret and Q bands are located at 450 nm and 640–700 nm, respectively. In particular, the strong Q band at 690 nm is indicative of crystallinity.[5] According to wide-angle X-ray scattering experiments, BP crystals have π-π stacking along a direction nearly parallel to the substrate.[5] In contrast, the BP:PCBM BHJ film has a weaker Q band at 675 nm, suggesting disordered π-π stacking of the BP.

Figure 2 plots a typical THz electric field transmitted through a sample in the absence of photo-excitation, together with an optical pump-induced differential field. With 400-nm photoexcitation, the amplitude of the photo-induced differential signal is generally less than 1% of the peak transmission of the THz probe pulse. Figure 3 displays the photo-induced change of the THz electric field amplitude as a function of the

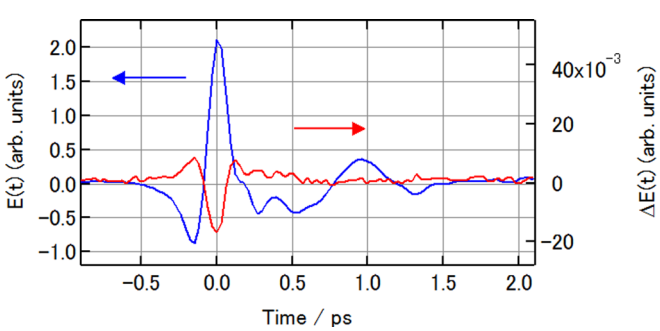

FIG. 2. THz electric field transmitted through a BP film without photo-excitation (blue), and the optically pumped induced differential THz electric field measured at a 0.4 ps time delay (red).

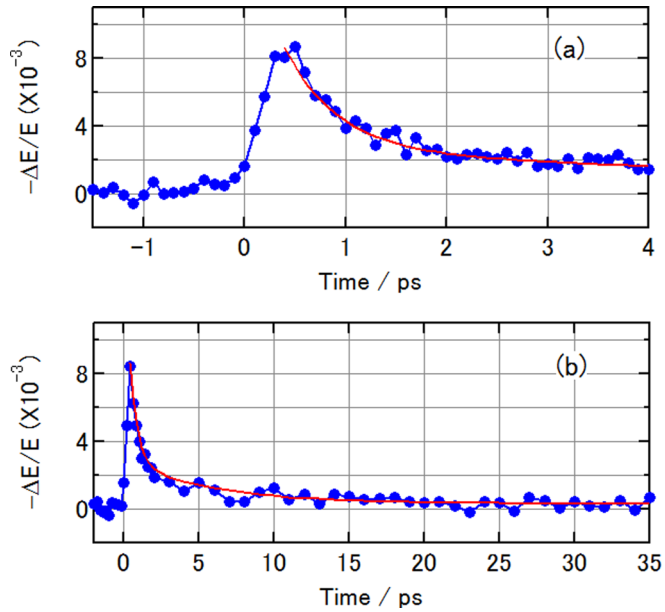

FIG. 3. (a) Photo-induced change of THz electric field amplitude in BP films as a function of optical pump/THz probe delay time, measured at the peak of the THz transmission. (b) Same as (a), except longer time scale. The excitation wavelength is 400 nm. Blue solid lines with filled circles and red lines represent the experimental results and double-exponential fits, respectively.

optical pump/THz probe delay time measured at the peak of the THz transmission and for a 530-μJ/cm^2 excitation intensity. The transient signal instantaneously decreases, followed by signal decays with time constants of 0.5 ± 0.1 ps and 6.0 ± 1.6 ps.[32] In this scan mode, the signal time dependence reflects the average BP photoconductivity. (In the supplementary material, we examined the excitation fluence-dependence of the photo-induced change in the THz electric field at the peak of the THz transmission.[32]) The frequency-dependent conductivity was extracted from the temporal profile of the THz electric field at a specific pump delay, with and without photoexcitation. In the thin film approximation, the sheet photoconductivity spectrum is given by

$$\frac{\tilde{\sigma}(\omega,T)}{N_{ex}} = -\frac{n_{air}+n_{quartz}}{Z_0}\frac{\Delta\tilde{E}(\omega,T)}{\tilde{E}_0(\omega,T)}, \tag{1}$$

where Z_0 is the impedance of free space (377 Ω), and n_{air} (1) and n_{quartz} (1.95) are the THz refractive indices of air and quartz, respectively.[11,34] It should be noted that the sheet conductivity is that value induced by a single photon and does not depend on the sample depth.[18]

Figure 4 plots the transient complex conductivity spectra measured at 0.4-ps and 1.2-ps delay times. The real parts of the spectra increase at high frequencies and have positive values at low frequencies, which suggest that the mobile charge carriers dominate the response in the THz region. The imaginary part of the conductivity is negative and approaches zero at a low frequency, which is different from that expected from the classical Drude model. Generally, the conductivity spectra in disordered systems can be described by the Drude–Smith model[35,36]

$$\tilde{\sigma}_{DS}(\omega) = \frac{\omega_p^2\varepsilon_0\tau}{1-i\omega\tau}\left(1+\frac{c}{1-i\omega\tau}\right), \tag{2}$$

Reuse of AIP Publishing content is subject to the terms at: https://publishing.aip.org/authors/rights-and-permissions. IP: 133.30.52.203 On: Mon, 22 Feb 2016 02:05:38

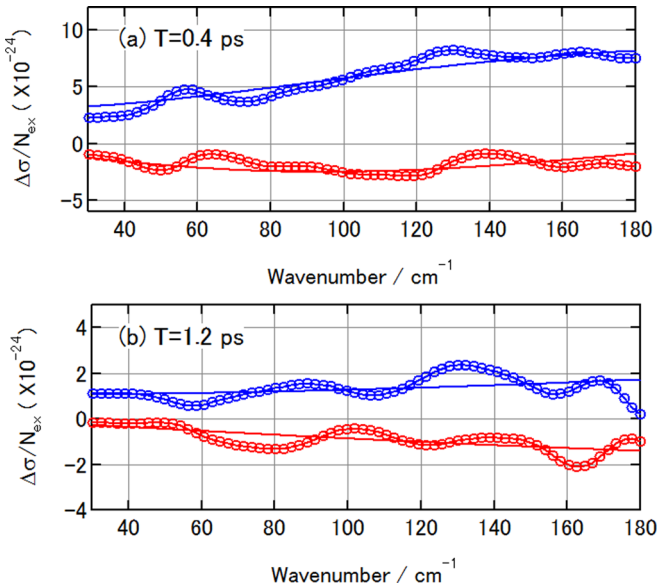

FIG. 4. Transient complex conductivity spectra of BP films measured at (a) 0.4 ps and (b) 1.2 ps. Blue (red) open circles are the real (imaginary) parts of the experimental transient conductivity. The corresponding solid lines are fits to the Drude–Smith model.

where ε_0 is the vacuum permittivity, ω_p is the plasma frequency, and τ is the carrier momentum relaxation time. (Note that this equation is expressed in terms of volume conductivity.) The effect of the disorder is described by the parameter c, which is related to the memory effect during the carrier scattering process. When $c = 0$, Eq. (2) describes the Drude model, where the carriers lose memory of the velocity and the momentum is randomized during scattering. For $c < 0$, the backscattered carriers are localized. To fit the data, we used the following equation by taking the excitation density into account:[18,34]

$$\frac{\tilde{\sigma}_{DS}(\omega)}{N_{ex}} = \frac{\omega_p^2 \varepsilon_0}{N_{ex}} \frac{\tau}{1 - i\omega\tau}\left(1 + \frac{c}{1 - i\omega\tau}\right) = \frac{\varphi e^2}{m^* d} \frac{\tau}{1 - i\omega\tau}\left(1 + \frac{c}{1 - i\omega\tau}\right), \quad (3)$$

where φ is the carrier quantum yield of the photon, m^* is the effective mass of the charge carrier, and d is the absorption depth. Since φ and m^* are unknown, we treat the first factor of the last expression in Eq. (3) as a proportional constant. Thus, we can only determine c and the carrier momentum relaxation time τ. We found that τ and c at 0.4 (1.2) ps are 21 ± 1 (6 ± 2) fs and -0.83 ± 0.01 (-0.89 ± 0.01), respectively.

Figure 5 shows the photo-induced change of the THz electric field amplitude in BP:PCBM BHJ films and the transient complex conductivity spectra for a 880-μJ/cm^2 excitation fluence and a 0.4-ps delay. The photo-induced change in the BHJ film is smaller than that in the BP film, even at higher excitation fluence, because PCBM itself absorbs 400 nm photons. Similar to the BP films, the transient signal decays with time constants of 0.2 ± 0.1 ps and 2.9 ± 0.5 ps. About one-tenth of the signal does not decay within 35 ps. The τ and c parameters in the Drude–Smith model for a 0.4-ps delay are 9 ± 1 fs and -0.87 ± 0.01, respectively.

As in Fig. 3, the THz transients show up immediately after photo-excitation because of the instantaneous appearance of mobile charge carriers. Exciton absorption is not possible, because it requires much higher transition energy (mid-infrared to visible), which does not appear in the THz transients. Previous studies suggested that the excess energy of hot excitons facilities charge separation that produces hot charge carriers very efficiently.[37,38] The energy gap between the highest occupied molecular orbitals and the lowest unoccupied molecular orbitals for BP is approximately 1.7 eV. Thus, photoexcitation at 400 nm (3.1 eV) produces an excess energy of 1.4 eV that may induce exciton dissociation into charge carriers.[7] Generated electrons and holes are separated but initially close to each other.

The rapidly decaying components in the observed signals have several possible origins because the sheet photoconductivity spectra are products of the charge carrier densities and their mobility spectra.[18] First, we note that early THz transients result from a reduction in carrier mobility as hot carriers thermally relax. Lane *et al.* reported that short-lived components of THz signals are caused by decreasing mobility as the carriers localize.[28] This is consistent with the transient complex conductivity spectra observed at 0.4 ps delay, because

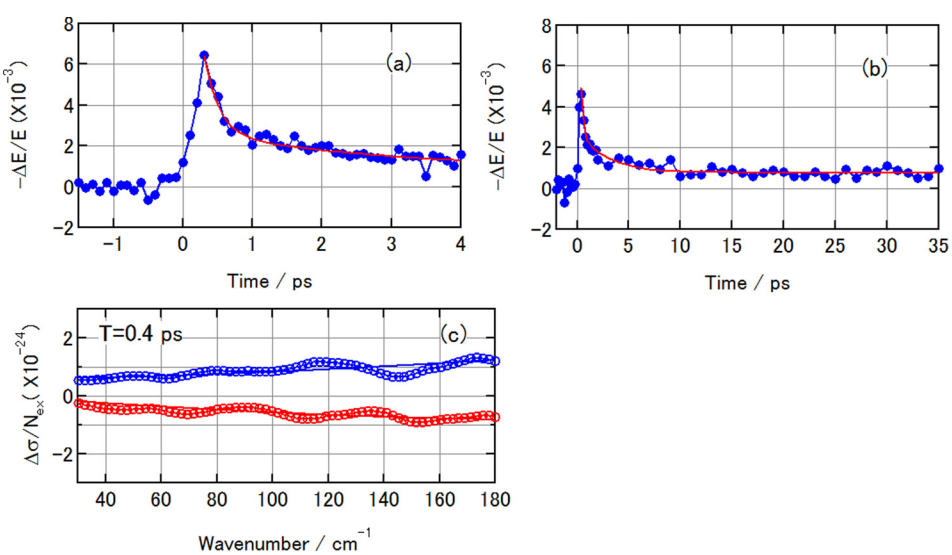

FIG. 5. (a) Photo-induced change of THz electric field amplitude in BP:PCBM BHJ films measured at the peak of the THz transmission. (b) Same as (a), except longer time scale. (c) Transient complex conductivity spectra of BP:PCBM BHJ films measured at 0.4 ps delay. Blue (red) open circles are the real (imaginary) parts of experimental transient conductivity. The corresponding solid lines are fits using the Drude–Smith model.

Reuse of AIP Publishing content is subject to the terms at: https://publishing.aip.org/authors/rights-and-permissions. IP: 133.30.52.203 On: Mon, 22 Feb 2016 02:05:38

the charge carriers undergo backscattering according to the Drude–Smith model. A second scenario is that the decay components derive from exciton formation, as reported for P3HT/PCBM BHJ films.[39] Further investigations of the excitation wavelength dependence will help to understand the origins of the sub-ps decaying components. In contrast, the slower decaying components in the THz transients are from recombination, and/or trapping at defect sites, of mobile charge carriers, that occur at the ps time scale.

In previous studies of pentacene and its derivatives, Ostroverkhova *et al.* observed Drude-like photoconductivity in both single crystals and thin films.[22,24] This differs from our observations. The average grain size in pentacene thin films was approximately 0.7–1.2 μm, depending slightly on the substrate.[25] Lima *et al.* reported that the grain sizes are about 150–200 nm in width and 150–1000 nm in length for thermally converted BP thin films.[5] It is therefore important in future work to see how crystal sizes and morphologies affect photoconductivity in BP thin films.

Jepsen *et al.* used time-resolved THz spectroscopy with broadband THz probe pulses to observe formation of mobile charges in P3HT:PCBM BHJ films.[39] Furthermore, they used the Drude–Smith model to fit the transient photoconductivity on a 200 fs time scale. Their τ and c parameters are similar to ours, even though the electronic structures are very different. Monomer units in conjugated polymers bond covalently and electrons delocalize along the π-conjugated backbone. Thus, conformational disorder affects the degree of exciton localization. In BP films, however, variations in the crystal structure and local morphology affect charge-carrier transport. In contrast to time-of-flight techniques that use electrical contacts, time-resolved THz spectroscopy can monitor the carrier mobility over nanometer length scales.[11,40,41] Thus, it may not be as sensitive to BP-films crystal sizes and grain boundaries.

Compared with the BP films, we observed faster (ps timescale) decay dynamics in the BP:PCBM BHJ films. This may be because they are less crystalline, they have smaller crystal domain sizes, and they have more defect sites based on the results of surface morphology by atomic force microscopy.[7] Therefore, charge carrier localization and recombination, and/or trapping, of mobile charge carriers can be faster. However, because 10% of the transient signal does not decay within 35 ps, a small portion of mobile charge carriers appears to survive. This is not consistent with the very low (0.02%) power conversion efficiency of the BP:PCBM BHJ film.[7] It should be noted that our sample preparations for the above measurements are different from those used for device characterization.[7] For current measurements, we have to increase the concentration of the BP:PCBM blends and change the temperature of the thermal conversion process of the precursor molecules to measure transient signals with a good signal-to-noise ratio. To determine the internal photon-to-carrier quantum yields for the BP and BP:PCBM BHJ films, it is necessary to know the effective mass of the carriers. Further studies concerning the above issues would provide more detailed insights on the formation and recombination dynamics of the charge carriers generated by photoexcitation.

In summary, we performed optical pump-THz probe measurements of charge-carrier dynamics in BP and BP:PCBM BHJ films. We found that the transient signals in BP films decay with time constants of 0.5 ps and 6.0 ps. Rapidly decaying components show up because of either reduced charge-carrier mobility or exciton formation. Slower decays originate from mobile charge carrier recombination and/or trapping at defect sites. Conductivity spectra can be fit by the Drude–Smith model, indicating that charge carriers localize within a picosecond. From comparison of the dynamics between the BP and BP:PCBM BHJ films, we consider that the degree of crystalline may affect charge carrier localization and recombination, and/or trapping, of mobile charge carriers.

This research was supported by an Industry-Academia Collaborative R&D program from the Japan Science and Technology Agency. This work was partly supported by Grants-in-Aid for Scientific Research (KAKENHI) Nos. 25288092 and 26105004 from the Japan Society for the Promotion of Science (JSPS).

[1]C. J. Brabec, S. Gowrisanker, J. J. M. Halls, D. Laird, S. Jia, and S. P. Williams, Adv. Mater. **22**, 3839 (2010).
[2]L. Dou, J. You, Z. Hong, Z. Xu, G. Li, R. A. Street, and Y. Yang, Adv. Mater. **25**, 6642 (2013).
[3]H. Yamada, T. Okujima, and N. Ono, Chem. Commun. **26**, 2957 (2008).
[4]Y. Matsuo, Y. Sato, T. Niinomi, I. Soga, H. Tanaka, and E. Nakamura, J. Am. Soc. Chem. **131**, 16048 (2009).
[5]D. Lima, S. Choi, D. W. Breiby, J. E. Cochran, M. F. Toney, E. J. Kramer, and M. L. Chabinyc, J. Phys. Chem. B **117**, 14557 (2013).
[6]M. Guide, X.-D. Dang, and T.-Q. Nguyen, Adv. Mater. **23**, 2313 (2011).
[7]Y. Tamura, H. Saeki, J. Hashizume, Y. Okazaki, D. Kuzuhara, M. Suzuki, N. Aratani, and H. Yamada, Chem. Commun. **50**, 10379 (2014).
[8]T. M. Clarke and J. R. Durrant, Chem. Rev. **110**, 6736 (2010).
[9]C. J. Babec, G. Zerza, G. Cerullo, S. De Silvestri, S. Luzzati, J. C. Hummelen, and S. Sariciftci, Chem. Phys. Lett. **340**, 232 (2001).
[10]I.-W. Hwang, D. Moses, and A. J. Heeger, J. Phys. Chem. C **112**, 4350 (2008).
[11]R. Ulbricht, E. Hendry, J. Shan, T. F. Heinz, and M. Bonn, Rev. Mod. Phys. **83**, 543 (2011).
[12]M. C. Beard, G. M. Turner, and C. A. Schmuttenmaer, Phys. Rev. B **62**, 15764 (2000).
[13]E. Hendry, M. Koeberg, J. M. Schins, H. K. Nienhuys, V. Sundstorm, L. D. A. Siebbleles, and M. Bonn, Phys. Rev. B **71**, 125201 (2005).
[14]X. Ai, M. C. Beard, K. P. Knutsen, S. E. Shaheen, G. Rumbles, and R. J. Ellingson, J. Phys. Chem. B **110**, 25462 (2006).
[15]O. Esenturk, J. S. Melinger, and E. J. Heilweil, J. Appl. Phys. **103**, 023102 (2008).
[16]P. D. Cunningham and L. M. Hayden, J. Phys. Chem. C **112**, 7928 (2008).
[17]P. Parkinson, J. Lloyd-Hughes, M. B. Johnston, and L. M. Hetz, Phys. Rev. B **78**, 115321 (2008).
[18]H. Nemec, H.-K. Nienhuys, F. Zhang, O. Inganas, A. Yartsev, and V. Sundstrom, J. Phys. Chem. C **112**, 6558 (2008).
[19]C. S. Ponseca, Jr., A. Yartsev, E. Wang, M. R. Andersson, D. Vithanage, and V. Sundstrom, J. Am. Chem. Soc. **134**, 11836 (2012).
[20]G. M. Turner, M. C. Beard, and C. A. Schmuttenmaer, J. Phys. Chem. B **106**, 11716 (2002).
[21]R. L. Milot and C. A. Schmuttenmaer, Acc. Chem. Res. **48**, 1423 (2015).
[22]F. A. Hegmann, R. R. Tykwinski, K. P. H. Lui, J. E. Bullock, and J. E. Anthony, Phys. Rev. Lett. **89**, 227403 (2002).
[23]V. K. Thorsmolle, R. D. Averitt, X. Chi, D. J. Hilton, D. L. Smith, A. P. Ramirez, and A. J. Taylor, Appl. Phys. Lett. **84**, 891 (2004).
[24]O. Ostroverkhova, D. G. Cooke, S. Shcherbyna, R. F. Egerton, F. A. Hegmann, R. R. Tykwinski, and J. E. Anthony, Phys. Rev. B **71**, 035204 (2005).
[25]O. Ostroverkhova, S. Shcherbyna, D. G. Cooke, R. F. Egerton, F. A. Hegmann, R. R. Tykwinski, S. R. Parkin, and J. E. Anthony, J. Appl. Phys. **98**, 033701 (2005).

Reuse of AIP Publishing content is subject to the terms at: https://publishing.aip.org/authors/rights-and-permissions. IP: 133.30.52.203 On: Mon, 22 Feb 2016 02:05:38

[26]O. Esenturk, J. S. Melinger, P. A. Lane, and E. J. Heilweil, J. Phys. Chem. C **113**, 18842 (2009).
[27]P. A. Lane, P. D. Cunningham, J. S. Melinger, G. P. Kushto, O. Esenturk, and E. J. Heilweil, Phys. Rev. Lett. **108**, 077402 (2012).
[28]P. A. Lane, P. D. Cunningham, J. S. Melinger, O. Esenturk, and E. J. Heilweil, Nat. Commun. **6**, 7558 (2015).
[29]D. J. Cook and R. M. Hochstrasser, Opt. Lett. **25**, 1210 (2000).
[30]J. Dai, J. Liu, and X.-C. Zhang, IEEE J. Sel. Top. Quantum Electron. **17**, 183 (2011).
[31]N. Karpowicz, J. Dai, X. Lu, Y. Chen, M. Yamaguchi, H. Zhao, X.-C. Zhang, L. Zhang, C. Zhang, M. Price-Gallagher, C. Fletcher, O. Mamer, A. Lesimple, and K. Johonson, Appl. Phys. Lett. **92**, 011131 (2008).
[32]See supplementary material at http://dx.doi.org/10.1063/1.4934690 for the details of the setup for time-resolved THz spectrometer, the fitted parameters of the one-dimensional transient signals, and excitation fluence dependence of photo-induced change of the THz electric field at the peak of the THz transmission.
[33]J. T. Kindt and C. A. Schmuttenmaer, J. Chem. Phys. **110**, 8589 (1999).
[34]Z. Jin, D. Cehrig, C. Dyer-Smith, E. J. Heilweil, F. Laquai, M. Bonn, and D. Turchinovich, J. Phys. Chem. Lett. **5**, 3662 (2014).
[35]N. V. Smith, Phys. Rev. B **64**, 155106 (2001).
[36]J. Lloyd-Hughes and T.-I. Jeon, J. Infrared, Millimeter, Terahertz Waves **33**, 871 (2012).
[37]G. Grancini, M. Maiuri, D. Fazzi, A. Petrozza, H. J. Egelhaaf, D. Brida, G. Cerullo, and G. Lanzani, Nat. Mater. **12**, 29 (2013).
[38]A. E. Jailaubekov, A. P. Willard, J. R. Tritsch, W.-L. Chan, N. Sai, R. Gearba, L. G. Kaake, K. J. Williams, K. Leung, P. J. Rossky, and X.-Y. Zhu, Nat. Mater. **12**, 66 (2013).
[39]D. G. Cooke, F. C. Krebs, and P. U. Jepsen, Phys. Rev. Lett. **108**, 056603 (2012).
[40]R. Mauer, M. Kastler, and F. Laquai, Adv. Funct. Mater. **20**, 2085 (2010).
[41]A. Kokil, K. Yang, and J. Kumar, J. Polym. Sci., Part B **50**, 1130 (2012).

Reuse of AIP Publishing content is subject to the terms at: https://publishing.aip.org/authors/rights-and-permissions. IP: 133.30.52.203 On: Mon, 22 Feb 2016 02:05:38